

Monitoring, analysis and spatial and temporal zoning of air pollution (carbon monoxide) using Sentinel-5 satellite data for health management in Iran, located in the Middle East

Vahid Safarianzengir, Behrouz Sobhani, Mohammad Hasan Yazdani & Mohammadkia Kianian

Air Quality, Atmosphere & Health
An International Journal

ISSN 1873-9318

Air Qual Atmos Health
DOI 10.1007/s11869-020-00827-5



Your article is protected by copyright and all rights are held exclusively by Springer Nature B.V.. This e-offprint is for personal use only and shall not be self-archived in electronic repositories. If you wish to self-archive your article, please use the accepted manuscript version for posting on your own website. You may further deposit the accepted manuscript version in any repository, provided it is only made publicly available 12 months after official publication or later and provided acknowledgement is given to the original source of publication and a link is inserted to the published article on Springer's website. The link must be accompanied by the following text: "The final publication is available at link.springer.com".



Monitoring, analysis and spatial and temporal zoning of air pollution (carbon monoxide) using Sentinel-5 satellite data for health management in Iran, located in the Middle East

Vahid Safarianzengir¹ · Behrouz Sobhani¹ · Mohammad Hasan Yazdani¹ · Mohammadkia Kianian²

Received: 31 March 2020 / Accepted: 8 April 2020
© Springer Nature B.V. 2020

Abstract

Various natural and anthropogenic factors are effective in causing air pollution. The effects of air pollution are more pronounced on the health of living things, especially on the mental and physical health. Therefore, this issue is important because of the importance of health and well-being. The purpose of the present study is to investigate the spatial and temporal monitoring and analysis of air pollution (carbon monoxide, CO) using satellite and remote sensing data in Iran. To do this, Sentinel-5 satellite data for air pollution (CO) monitoring over a 14-month period (November 2018 to December 2019) and Terra satellite and MODIS satellite data with LST index for monitoring changes of daily and nocturnal temperatures (Kelvin unit) over a 24-month period (January 2018 to December 2019) were used. The results showed that the highest amount of air pollution (CO) was obtained in April 2019 with 0.39 mol/m². However, the highest amount of air pollution in spatial monitoring of CO was obtained for Tehran and Guilan provinces with values of 0.51 mol/m² and 0.49 mol/m² respectively, while the lowest amount of CO was 0.19 mol/m² for December 2019. Northwestern Iran, south and west areas of the central part of Ardebil province, south half and eastern part of East Azarbaijan province, Sahand mountain range, and western part of the border section of West Azerbaijan province were exposed to air pollution with average values of 0 to 0.21 mol/m². Since the highest amounts of air pollution (CO) occur during the cold months of the year, people who are vulnerable to this phenomenon should travel to the polluted sites with observing hygiene principles.

Keywords Air quality · Monitoring · Carbon monoxide · Crisis management · Remote sensing · Health · Pollutants

Introduction

Investigating the circadian, seasonal, and annual variations of various meteorological parameters has various applications, especially wind and air temperature in the surface layer of the urban atmosphere. For example, knowing how local wind

circulation systems are formed and how temperature changes during the day and in the season will help to identify conditions that lead to acute air pollution events (Vanino et al. 2018; Omrani et al. 2020; Sager 2019; Sobhani and Safarianzengir 2019a; Sobhani et al. 2019a, b). Investigating changes in the concentration of air pollutants, especially carbon monoxide (CO) and aerodynamic particles less than 5 µm in diameter (PM₁₀), is of particular importance in terms of its impact on human health and the environment. Identifying the circadian and seasonal variations of meteorological parameters and the factors influencing these changes such as topographic structure, urban heat islands, and large and mid-scale systems which create and enhance the stability of the air, inversion of temperature, low wind and changes in solar radiation; air pollutants and their correlation, identifying the sources, conditions and how pollutants are produced and released, and contributing to each of these sources in air pollution, enables the management of air pollution (Tiwary and Colls 2010; Kurata et al. 2020; Kristin et al. 2019; Sobhani et al. 2018; Safarianzengir et al. 2019). Complete and incomplete

✉ Vahid Safarianzengir
safarian.vahid@gmail.com

Behrouz Sobhani
sobhani@uma.ac.ir

Mohammad Hasan Yazdani
yazdani.m51@gmail.com

Mohammadkia Kianian
m_kianian@semnan.ac.ir

¹ Faculty of Literature and Humanities, University of Mohaghegh Ardabili, Ardabil, Iran

² Desert Studies Faculty, Semnan University, Semnan, Iran

combustion of fuel in vehicles using gasoline and diesel fuel creates a complex mix of gaseous and particulate pollutants, many of which are harmful to human health. As the commute rises, movement and stop and at the beginning of the journey (the first 2 to 3 km), which the car engine is cold, CO diffusion increases (Jeniffer et al. 2019; Li et al. 2020; Paola et al. 2019). The rate of emission of pollutants may be directly related to meteorological conditions (such as evaporation) or indirectly (such as increased use of heating devices in the cold months of the year) (Oanh et al. 2005; Cheung et al. 2020; Kurata et al. 2020; Li et al. 2020; Lu et al. 2019; Miller 2020; Omrani et al. 2020; John and Balmes 2019). Usually, the concentration of pollutants in direct urban environments is not due to directly increased pollutant emissions. Rather, it is the result of adverse weather conditions. These conditions may reduce the ability of the atmosphere to diffuse contaminants and transfer them from contamination sources to other areas or be a combination of the two above (Lalas et al. 1980; Schikowski and Altug 2020; Moon 2019; Safarianzengir and Sobhani 2020; Sobhani and Safarianzengir 2020). Also, the study of the meteorological conditions that caused air pollution over the central Po (Po) valley showed that in all periods of air pollution, cyclones were dominant and in the middle troposphere, existed warm air (Sandro and Pellegrini 2004; Miller 2020; Julia et al. 2019). The issue of air pollution in major cities has been exacerbated by concerns over the past few decades due to the presence of numerous polluting sources such as automobiles, industries, heating devices, construction, and commercial activities (Ibbetson et al. 2020; Song et al. 2019). The structure and local characteristics of air pollution in a city, on the one hand, are influenced by human activities and energy consumption due to the high density of the urban population and on the other hand, are related to the natural system governing the region, in particular, the physiographic structure and local and regional atmospheric circulation (Fan et al. 2020; Fouladi et al. 2020; Golbaz et al. 2009; Ibbetson et al. 2020; Rohi et al. 2020; Lu et al. 2019; Sobhani et al. 2020a, c; Sobhani and Safarianzengir 2019b).

Accordingly, the emergence of air pollution in urban space and the extent of its location can not only be explained in terms of citizens' lifestyle, urban community behavior, and the type and quality of the human activity but also for any polluted urban activity center a complex combination such as natural and anthropogenic factors play a role in determining the characteristics and structure of local and regional air pollution (Wu and Lu 2020; Joris and Ommeren 2020; Sobhani et al. 2020b). In the meantime, the emergence of heavily polluted days associated with critical pollution conditions is of metropolitan properties, which has a very wide negative impact on the inhabitants of these cities and the urban environment in general (Fouladi et al. 2020; Fan et al. 2020). The occurrence of extreme pollution in urban air and the emergence of critical conditions in the concentration of

atmospheric pollutants is a phenomenon that has occurred in the metropolitan areas of Iran in recent years and has had wide negative effects. MODIS sensor data can be used to obtain much information such as temperature and humidity, pollutions, cloud cover, ice and snow distribution and depth, ocean color, vegetation indices, land and sea surface temperature, fire, and natural and anthropogenic burns (Wang et al. 2010; Govender and Sivakumar 2020). Therefore, with a review of past research work, the necessity of this research is discussed here. Nazarian et al. (2007) studied the role of morphological location in Tehran air quality and concluded that the method used is based on remote sensing thermal optical data that is possible to map the Tehran metropolitan surface temperature and the distribution of co-pollutants on it. Ghorbani et al. (2010) studied the ability of MODIS sensing data to perform qualitative and quantitative analyses of air quality in urban areas and found that the data obtained and measured at ground-based station of pollution monitoring can only be cited within a limited radius of their surroundings, and the accuracy of MODIS's air pollution monitoring data was acceptable. Ghorbani et al. (2012) carried out a rapid method of estimating suspended particulate matter concentration using a MODIS's sensor in Tehran and concluded that the existence of dependence between remote sensing calculations and ground measurements indicates that satellite imagery is applicable to monitor the status of contaminants in urban areas. Shamsipour and Amini (2013) simulated the CO distribution pattern and found that the maximum concentration of contamination in sections with urban texture density such as Valiasr intersection and south side of Tehranpars and remote areas especially in mid-day. Saghafi and Aliakbari (2014) investigated the circadian and seasonal variations of wind, air temperature, and CO and PM₁₀ pollutants in the surface layer of Tehran's atmosphere and concluded that both components of wind speed and temperature play a role in PM₁₀ transmission. Soltani et al. (2015) studied the synoptics of highly polluted days in Mashhad and found that the pattern of simultaneous formation of low-thickness inversion layers is below 400 hPa. Mozaffari et al. (2015) analyzed the relationship between synoptic patterns with particulate matter and carbon monoxide pollutants in Shiraz and concluded that the trend of carbon monoxide concentration was decreasing over the period. Kabolizadeh et al. (2000) studied the application of a combination of Landsat-8 and Sentinel-2 satellite images in environmental monitoring and found that the highest spatial deviation in DWT index had a correlation value of 0.47 with the reference image. Rangzan et al. (2019) modelled and zoned water quality parameters using Sentinel-2 satellite images and ANFIS and artificial neural network model and found that sulfate ANFIS model with relative error and root mean square error (RMSe) 0.077 and 0.801 had more accuracy than artificial neural network model with relative error and RMSe 0.158 and 1.247. Due to the importance of the issue of air pollution,

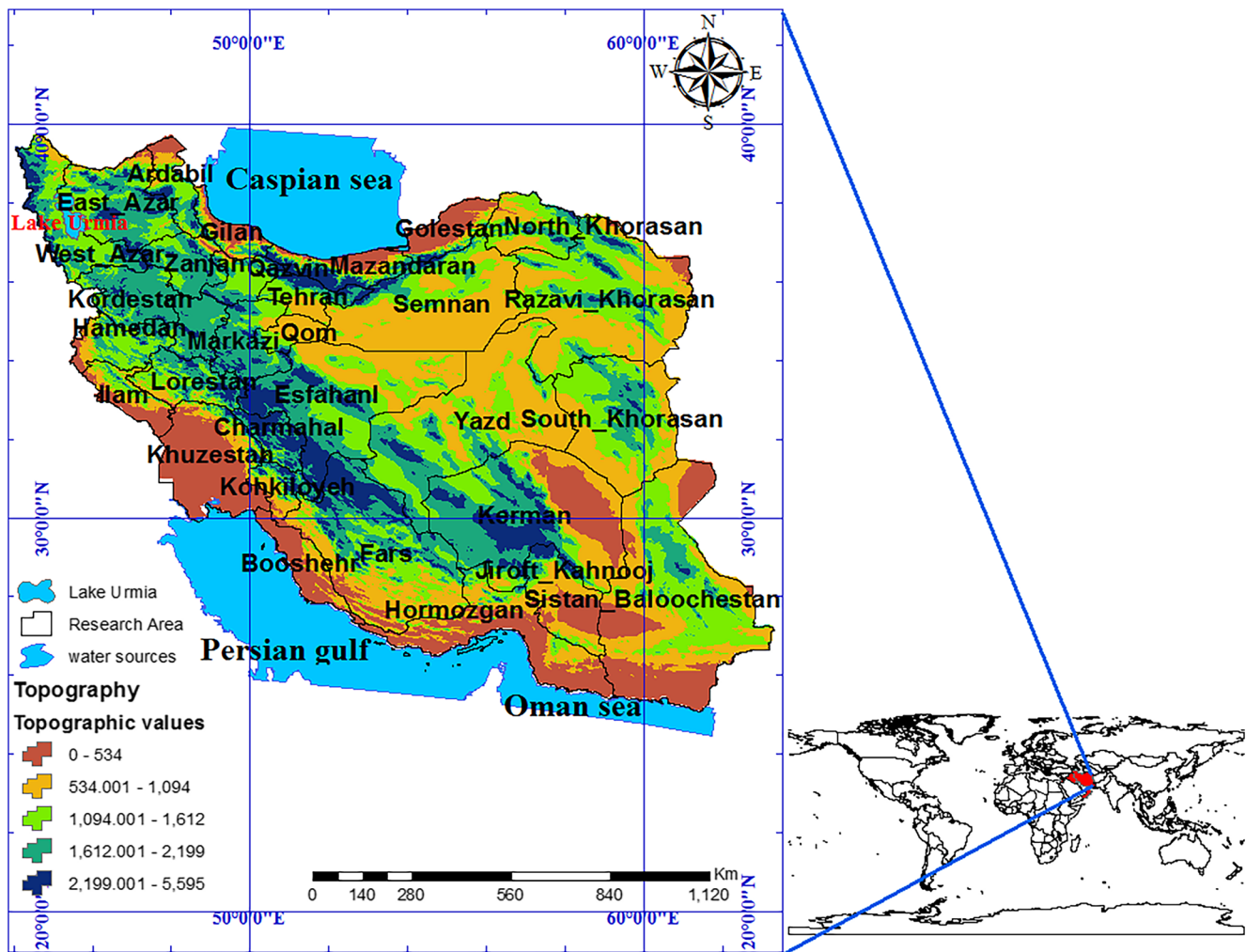


Fig. 1 Geographical location of the study area

many studies in Iran and abroad have been done by researchers. Most of them generally have used ground-based data for contamination monitoring although these data are limited to the location of the measuring stations and cannot adequately address the issue. It also cannot be expanded to more remote areas, and therefore, remote sensing data and valid methods and indices were used in this study. Considering the above issues, the purpose of this study is to monitor, analyze, and map the temporal and spatial extent of air pollution in the metropolitan areas of Iran.

including Terra-MODIS and Sentinel-5 satellite data for Iran. Sentinel-5 satellite data were used to monitor 14-month pollution changes (November 2018 to December 2019) and Terra satellite data were used to monitor daily and nocturnal temperature changes with the Kelvin unit over a 24-month period (January 2018 to December 2019). The study area is presented in Fig. 1.

Materials and methods

Study area

The purpose of this study was to study air pollution in Iran's metropolitan areas. For this purpose, some data were used

Table 1 Sentinel-5 satellite band specifications

Band name	Spectral range (nm)
Ultraviolet	270–320
Visible range	310–500
Near infrared	675–775
Short-wavelength infrared	2305–2385

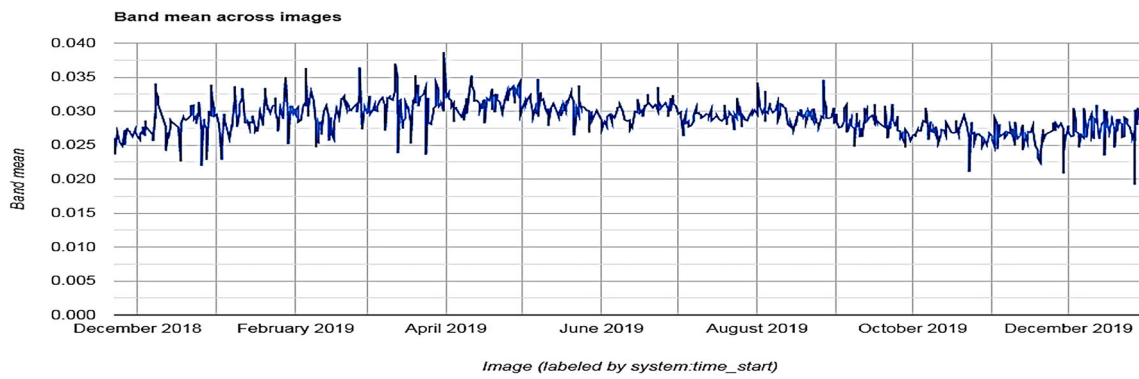


Fig. 2 Diagram of carbon monoxide changes in northern Iran over a 14-month period (November 2018 to December 2019)

Research methodology

Sentinel-5 satellite

The Sentinel-5 satellite (Copernicus Sentinel-5), launched on October 17 of 2017, is part of the Sentinel Fleet mission developed by the European Space Agency to monitor the European environment and monitor air pollutants around the globe. The satellite is tasked with monitoring pollutants such as carbon and nitrogen dioxide and ozone. The first mission of the Copernicus program for air pollution control is the construction of the Sentinel-5 sensor (Lesley et al. 2019). This sensor supports ultraviolet, visible, short infrared, and short-wavelength infrared bands. This satellite is at an altitude of 824 km and can be useful in detecting ozone, methane, formaldehyde, aerosol, carbon monoxide, NO₂, and SO₂. The characteristics of the Sentinel-5 bands are presented in Table 1 (Rohi et al. 2020; Sager 2019; Song et al. 2019; Purwadi et al. 2020).

Poor air quality is a serious health issue. Air pollution impacts equally the lives of people in developed and developing countries. It is estimated that only in Europe about 400,000 die annually due to poor air quality. The Earth Observation Programs Director of the European Space Agency (ESA) emphasizes that Sentinel-5 mission is a good example of

cooperation between European countries to benefit their citizens for using these data (Matthias et al. 2020). The Sentinel-5P satellite is a joint project between the European Space Agency (ESA) and the Netherlands operated by the Dutch Space Bureau. The satellite has a Tropospheric Monitoring Instrument that supports ultraviolet, visible, infrared, and short-wavelength infrared (Priya et al. 2020). The purpose of this satellite launch is to measure atmospheric layers with a very high spatial and temporal resolution that can measure air quality, atmospheric water pressure, ozone, and ultraviolet rays. It can also be useful in estimating gases such as sulfur dioxide, nitrogen dioxide, carbon monoxide, formaldehyde, and methane (Bart et al. 2020).

LST index

To calculate the LST (ground surface temperature) after preparing the images, the necessary pre-processing including ground reference MODIS satellite optical and thermal data with 1 × 1-km resolution, and luminosity temperature estimation for bands 31 and 32, this sensor was done. Because clouds and water have a low temperature and in the final maps assigned the minimum temperature, it was necessary to apply cloud and water removal algorithm to the images to meet the ground temperature thresholds related to the phenomena.

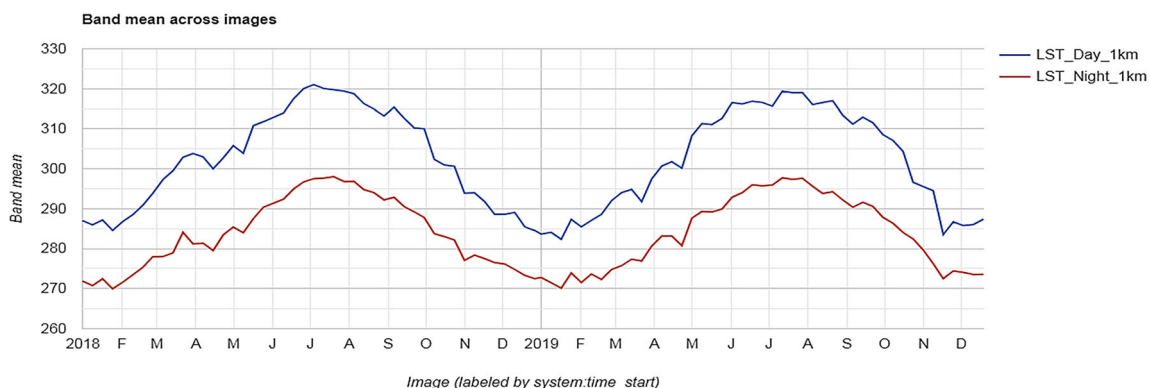


Fig. 3 Diagram of daily and nocturnal temperature changes in northern Iran over a 24-month period (January 2018 to December 2019)

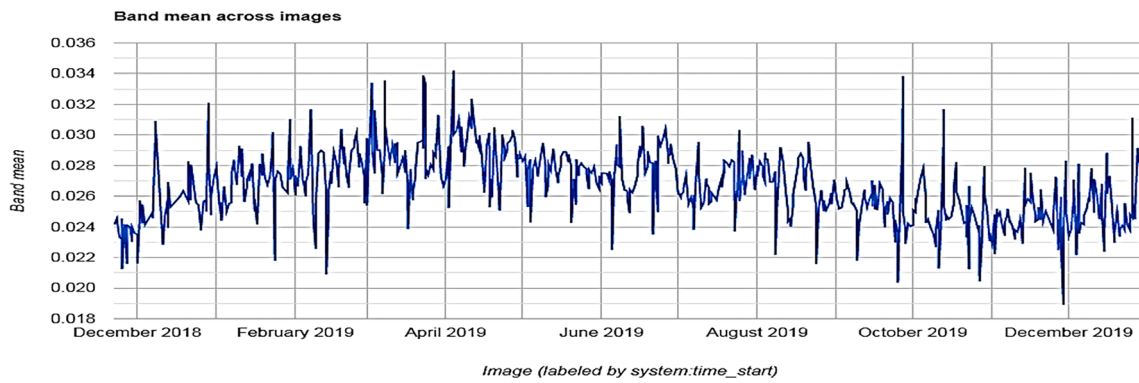


Fig. 4 Diagram of carbon monoxide changes in northwestern Iran over the 14-month period (November 2018 to December 2019)

Therefore, the cloud and water were removed from the images and the surface temperature was calculated using the algorithm proposed by Cole and Casillas (Kohavi and Provost 1998). MODIS images are taken daily from the two Aqua and Terra satellites at the Mahdasht Space Center. The LST product can be manufactured daily in the country. Due to the prevailing weather conditions in the country and cloudy weather in the cold months of the year, preparation of these maps is limited (Vanino et al. 2018; Wan 1999; Wu and Lu 2020; Susan et al. 2018). Overall accuracy was obtained by Eq. (1).

$$\text{Overall Accuracy} = \frac{\text{TP} + \text{TN}}{\text{TP} + \text{TN} + \text{FP} + \text{FN}} = \frac{\text{TP} + \text{TN}}{N} \quad (1)$$

Brightness temperature difference index (BTD)

The bands 4 (3.10–3.11 μm) and 5 (5.11–5.12 μm) of NOAA are in the infrared thermal window range, which the absorption is negligible by other atmospheric gases. In each of bands 4 and 5, the temperature difference between ground, dust, and cloud is high, but the dust has a higher temperature in band 5 than in band 4 against other phenomena. Therefore, bands 4 and 5 and the difference in the radiation temperature between the two bands can be used to detect the phenomenon of air pollution on the images. Radiation temperature is obtained by

converting the data of bands 4 and 5 using the Planck equation inverting (Wan 1999). The luminosity temperature, which is the temperature corresponding to the radiant energy received from the surface by the sensor and is calculated regardless of the emission, differs from the actual temperature and is obtained by inverting the Planck equation. The brightness temperature difference index is calculated by relation (2). This method was first used by Ackerman to detect dust in MODIS images, and he concluded that negative values of this indicator represent dust. In the AVHRR sensor, the indexes are also separated from the image with negative numerical values and the cloud with positive numerical values (Tsolmon et al. 2008).

$$\text{BTDI} = \text{Ch4} - \text{Ch5 by AVHRR/NOAA} \quad (2)$$

NDSI index

In this method, first, the dual-reflectance criteria (i.e., the reflectance value of the pixels in the six-band greater than 11% and the pixel-reflectance value in band 4 equal to or greater than 10%) and the condition of NDSI > 0.4 were applied according to Eq. 3 (Nolin and Liang 2000; Blosch and Parajka 2008). For the estimation of ground surface temperature (LST), the method of Sobrinu separate window algorithm was used. MOSTIS LST temperature map algorithm from

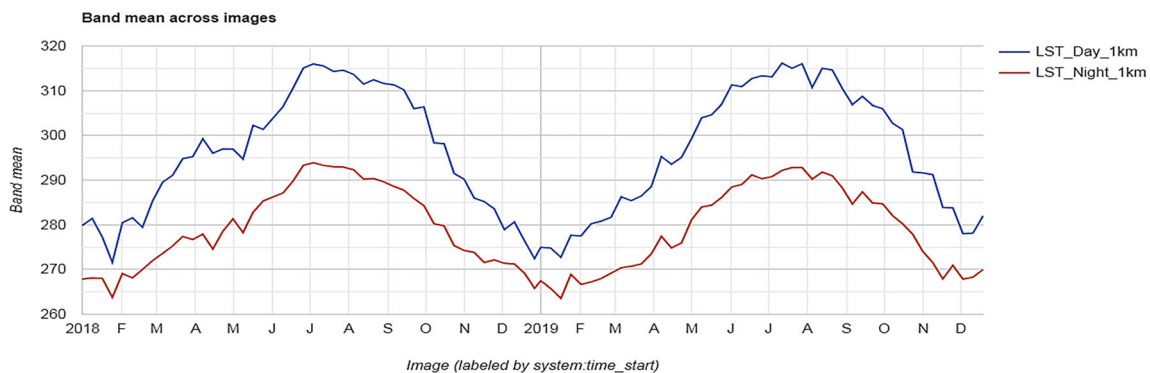


Fig. 5 Diagram of daily and nocturnal temperature changes in northwestern Iran over the 24-month period (January 2018 to December 2019)

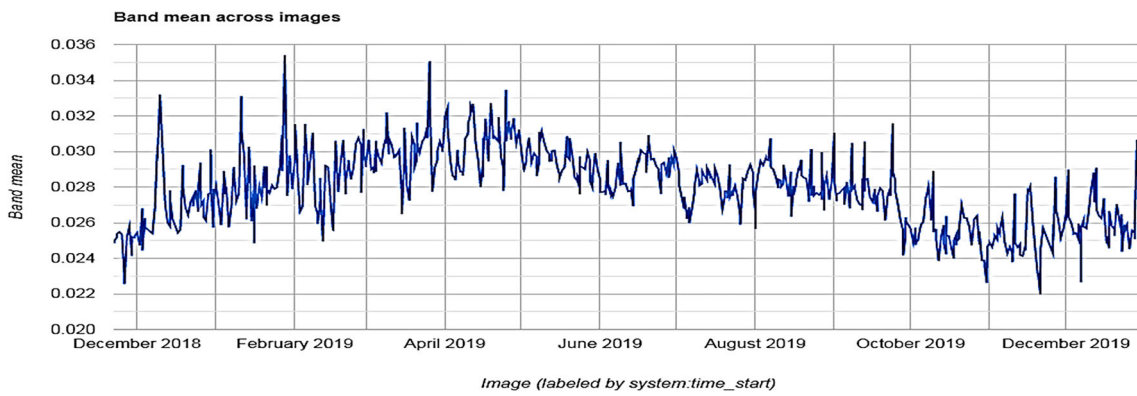


Fig. 6 Diagram of monoxide carbon changes in northeast of Iran over the 14-month period (November 2018 to December 2019)

bands 4 and 6 of this sensor automatically implemented to extract the differential thermal index (NDSI) and based on Eq. (3) was calculated (Emre et al. 2005).

$$NDSI = \frac{MODIS_{Band4} - MODIS_{Band6}}{MODIS_{Band4} + MODIS_{Band6}} = \frac{green - SWIR}{green + SWIR} \quad (3)$$

In the above relation, band 4 (0.545–0.665 μm) has a reflectance equal to or greater than 10%. Band 6 (0.841–0.876 μm) has a reflectance of more than 11%.

Results and discussion

According to the findings of air pollution in the north of the study area, the highest amount of carbon monoxide (CO) over the 14-month period (November 2018 to December 2019) in the northern region of Iran was obtained in February 2019 with a value of 0.37 mol/m² and in April of 2019 with a value of 0.39 mol/m² and the lowest amount of carbon monoxide (CO) in the study period in October 2019 with a value of 0.21 mol/m² and in December 2019 with a value of 0.19 mol/m² (Fig. 2). It is worth noting that due to the importance of daily temperature in increasing the quality of air pollution, the daily temperature was further discussed. The results

of monitoring the daily changes in night and daytime temperature over the study period over the 24-month period (January 2018 to December 2019) in the northern region of Iran have the highest temperature (Kelvin unit) for July with 320 K and August with 319 K in 2019. The lowest values obtained from monitoring the daily and nocturnal temperature changes in the study period in northern Iran were 261 K in January and 262 K in November, respectively (Fig. 3).

According to the findings in the study area, the highest amount of air pollution (carbon monoxide) was obtained in the colder months of the year, mainly due to the phenomenon of inversion or temperature inversion. Temperature inversion occurs when a layer of warm air is above the cold air adjacent to the ground surface. Under such conditions, air stability is achieved, and instead of decreasing temperature with increasing altitude, it will increase to several hundred meters above the ground with increasing altitude. The same temperature inversion plays a key role in air pollution, as it contributes to the stability of the atmosphere and, consequently, prevents the vertical movement of the pollutants. On the other hand, it destroys wind energy and thus prevents vertical and horizontal dispersion of pollutants. When such sources of air pollutants, such as cars and factories, continuously inject their pollutants into the surface layer, the concentration of the pollutants increases sharply and air pollution reaches its highest level when

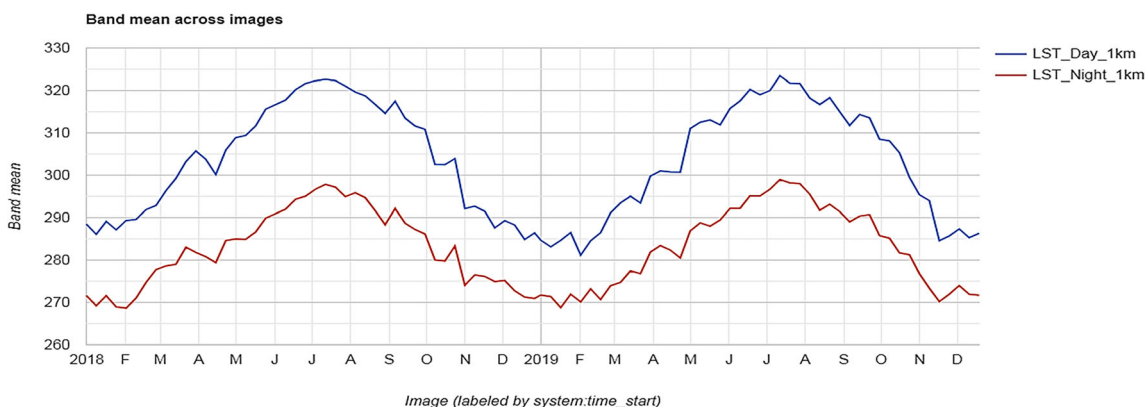


Fig. 7 Diagram of daily and nocturnal temperature changes in northeast of Iran over the 24-month period (January 2018 to December 2019)

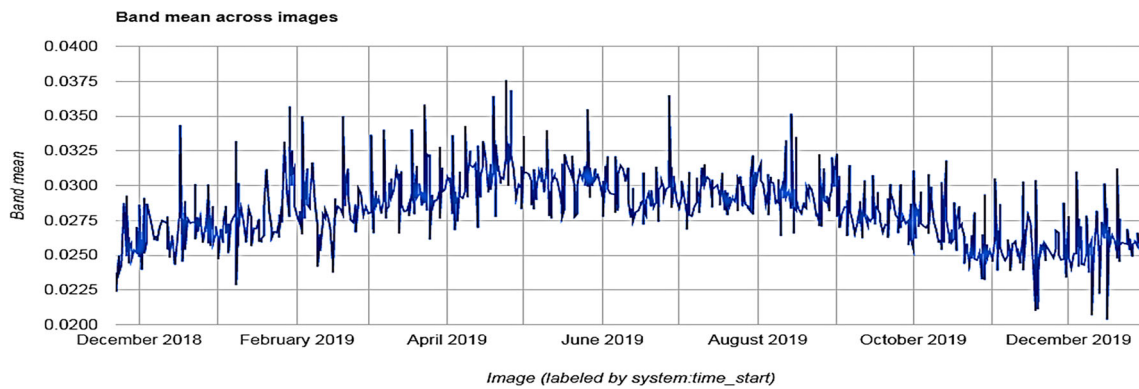


Fig. 8 Diagram of carbon monoxide changes in southwestern Iran over the 14-month period (November 2018 to December 2019)

the phenomenon of inversion occurs at low altitude and for longer periods in the city air, and this, of course, threatens human health.

According to the findings of air pollution in the northwest of the study area, the highest amount of carbon monoxide (CO) in the study period during the 14-month period (November 2018 to December 2019) in the northwestern region of Iran in April 2019 was obtained 0.34 mol/m^2 and in October 0.33 mol/m^2 and the lowest carbon monoxide (CO) in the study period in December was obtained 0.20 mol/m^2 and in August 0.21 mol/m^2 (Fig. 4). The results of monitoring the daily changes in night and daytime temperature over the 24-month period (January 2018 to December 2019) in the northwestern region of Iran have the highest temperature (Kelvin unit) for July with 315 K in 2019 and in August with 314 K in 2019. The lowest values from monitoring the daily and nocturnal temperature changes in the study period in the northwest of Iran were obtained 262 K in January and 263 K in February (Fig. 5).

According to the findings of air pollution in the northeast of the study area, the highest amount of carbon monoxide (CO) in the study period during the 14-month period (November 2018 to December 2019) in the northeast of Iran in January 2019 was obtained 0.35 mol/m^2 and in February, 0.34 mol/m^2 and lowest CO in the study period in October, 0.23 mol/m^2

and in December, 0.2 mol/m^2 (Fig. 6). The results of monitoring the daily changes in night and daytime temperature over the study period over the 24-month period (January 2018 to December 2019) in the northeast of Iran had the highest temperature (Kelvin unit) for June with 325 K in 2019 and for September 323 K. The lowest values obtained from monitoring the daily and nocturnal temperature changes in the study period in northeastern Iran were obtained 267 K in 2019 and 268 K in 2019 (Fig. 7).

According to the findings of air pollution in the southwest of the study area, the highest amount of carbon monoxide (CO) in the study period during the 14-month period (November 2018 to December 2019) in the southwestern region of Iran for April 2019 was obtained 0.38 mol/m^2 and for June, 0.36 mol/m^2 , and the lowest amount of carbon monoxide (CO) in the study period in October 2019 was obtained 0.22 mol/m^2 and in December, 0.21 mol/m^2 (Fig. 8). The results of monitoring the daily changes in night and daytime temperature over the study period over the 24-month period (January 2018 to December 2019) in the southwestern region of Iran had the highest temperature (Kelvin unit) for June with 323 K and for July 324 K in 2019. The lowest values from monitoring the daily and nocturnal temperature changes in the study period in southwestern Iran were obtained 281 K in January and 283 K in March 2019, respectively (Fig. 9).

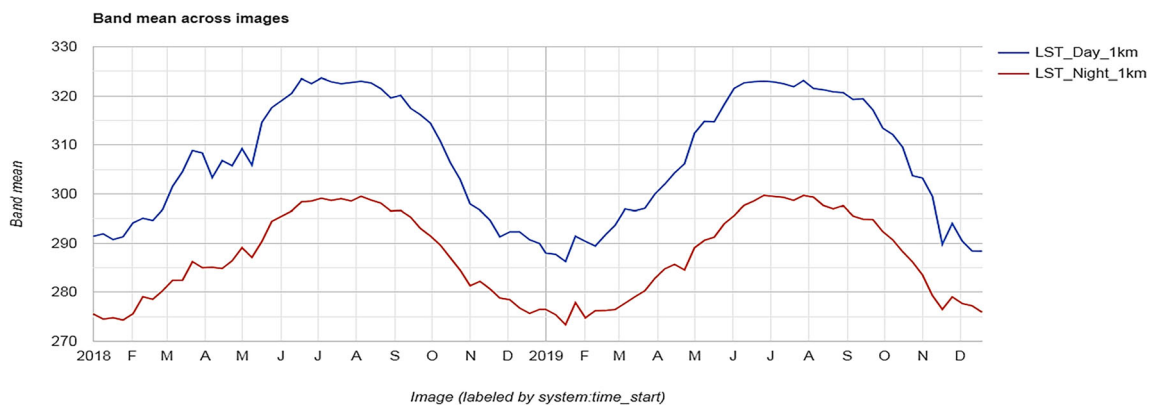


Fig. 9 Diagram of daily and nocturnal temperature changes in southwestern Iran over the 24-month period (January 2018 to December 2019)

According to Sentinel-5 satellite maps and satellite data for the monitoring of air pollution (carbon monoxide) over a 14-month period (November 2018 to December 2019) in the north of Iran, the area of Tehran province and Guilan province had the highest amounts of carbon monoxide with values of 0.51 mol/m^2 and 0.49 mol/m^2 , respectively, while in the western region, Qazvin, Guilan, and Qom; south half of Mazandaran and northwest of Semnan province had average values of 0 to 0.24 mol/m^2 (Fig. 10a). The results of air

pollution in the northwestern parts of Iran indicate that the central part had a rate of 0.34 mol/m^2 , and the northern part of Ardebil province had 0.32 mol/m^2 , the western part of Lake Urmia (Urmia city) had the amount of 0.28 mol/m^2 , north of West Azerbaijan province had the value of 0.31 mol/m^2 , and the semi-border part of North East Azerbaijan with 0.33 mol/m^2 had the highest amount of air pollution (carbon monoxide), while the south and west areas of the central part of Ardebil province, the southern half and eastern part of the eastern

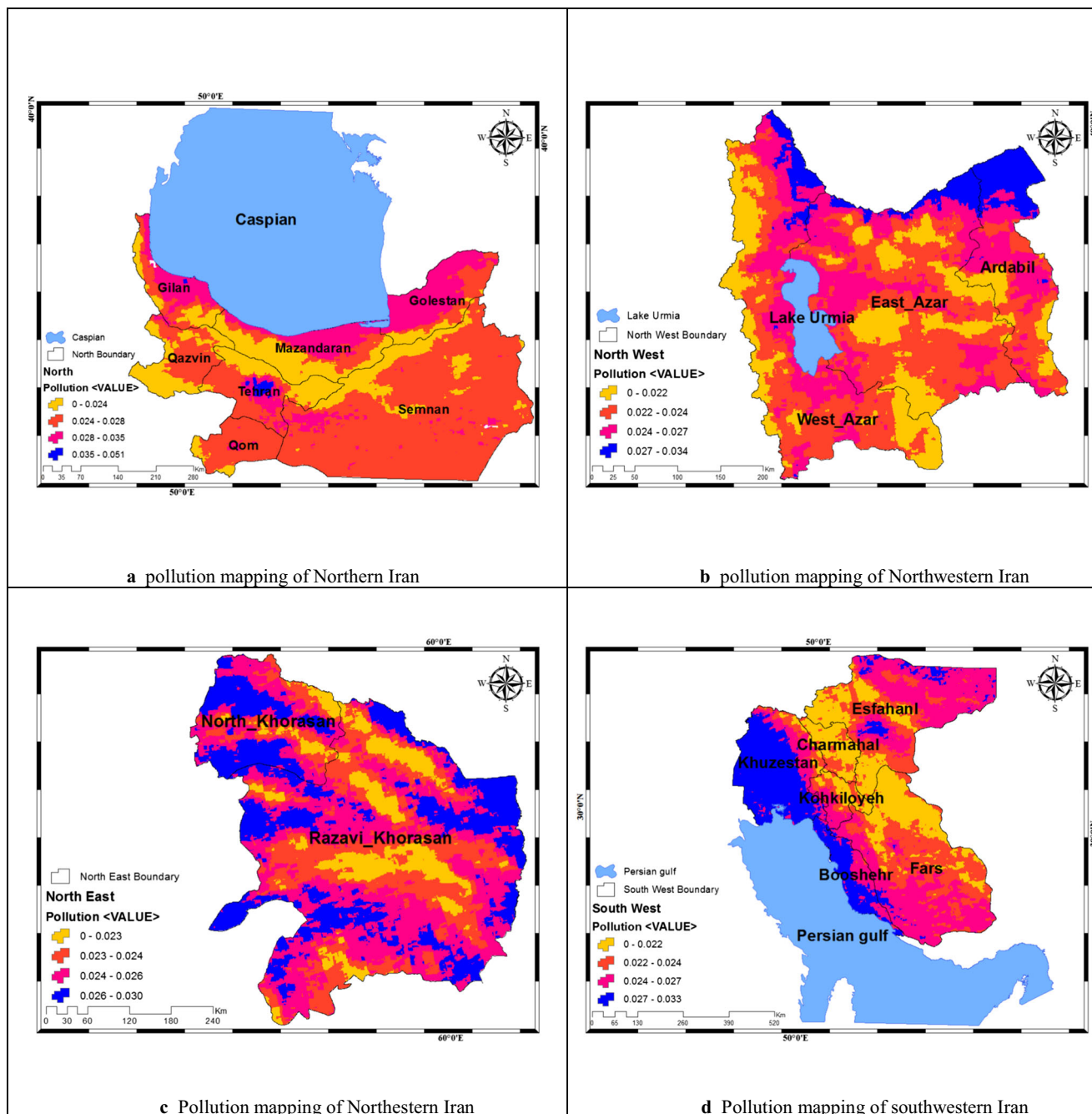


Fig. 10 Monitoring and mapping of air pollution (carbon monoxide) of the study areas over the 14-month period (November 2018 to December 2019). **a** Pollution mapping of northern Iran. **b** Pollution mapping of

northwestern Iran. **c** Pollution mapping of northeastern Iran. **d** Pollution mapping of southwestern Iran

Azərbaycan province, the border area of the Sahand mountain, the western part of the border part of the western Azerbaijan province had an average, amounts of 0 to 0.21 mol/m², indicating these parts had lower exposure to air pollution against the other parts (Fig. 10b). Findings from northeast of Iran indicate that the northern part had values of 0.30 mol/m² and the southern part had values of 0.28 mol/m² of North Khorasan province. The western part with 0.26 mol/m² and eastern part with 0.30 mol/m² of Khorasan Razavi province had the highest amount of air pollution. However, the eastern part of North Khorasan province and the central and northern part of Khorasan Razavi province with average carbon monoxide values of 0 to 0.23 mol/m² were less polluted compared with the other areas mentioned (Fig. 10c).

Finally, the results obtained from southwestern Iran indicate that a large part of the west of Khuzestan province with values of 0.33 mol/m²; sub-coastal Bushehr province with values of 0.32 mol/m²; southwest of Fars province with values of 29 mol/m²; and a central part with values of 0.33 mol/m² and northern strip with values of 0.31 mol/m² in Isfahan province were more exposed to air pollution (carbon monoxide). But the west and central part of Isfahan province; wide part of the northern half of Fars province, north of Chahar Mahal Bakhtiari province, and northeast part of Kohgiluyeh and Boyer-Ahmad province with mean carbon monoxide values of 0 to 0.22 mol/m² were less affected than other areas (Fig. 10d).

Conclusions

Human health is one of the most important issues globally and has been the focus of many governments. In recent decades, air pollution (carbon monoxide) has been one of the phenomena that has attracted much attention due to its destructive effects. Therefore, this issue is of great importance. The purpose of the present study is to investigate the spatial and temporal monitoring and analysis of air pollution (carbon monoxide, CO) in Iran. One of the innovations of the present study is the use of remote sensing data. The results showed that two regions of north and southwest of Iran with the following amounts of carbon monoxide (CO) in the study period over the 14-month period (November 2018 to December 2019) in February 2019 with 0.37 mol/m² and in April 0.39 mol/m² and northern Iran in April 2019 with 0.38 mol/m² and southwestern Iran in June with 0.36 mol/m² had the highest amount of air pollution. The minimum amount of carbon monoxide (CO) in the study period in October 2019 was 0.21 mol/m² and in the north of Iran in December was 0.18 mol/m². The temperature data also showed the highest temperature (Kelvin unit) for June with 325 K and September with 323 K in 2019 in northeastern Iran. The lowest amount was in January with 261 K and in November with 262 K in 2019 in the northern

part of Iran. According to the findings, the most contamination is in the cold months of the year. According to Sentinel-5 satellite data and zoning maps for the monitoring of air pollution (carbon dioxide) over a 14-month period (November 2018 to December 2019) in northern parts of Iran, Tehran and Gilan provinces had the highest amount of carbon monoxide with values of 0.51 mol/m² and 0.49 mol/m², respectively. In winter, residential areas are the most polluting source.

In this season, fuels such as diesel and gas are emitted from factories and homes, which are sources of pollution. It is also more intense than hot seasons due to the phenomenon of air inversion. But summer pollutants are far more dangerous to human health than winter pollutants because nitrogen- and sulfur-based pollutants that get out of cars are in lower parts of the atmosphere in summer and affect human health. The effects of air pollution, which can be mentioned in the study area, are as below: children with respiratory diseases, as air pollution increase children with a history of lung disease. Motor vehicle traffic and home heating systems are the biggest contributors to air pollution in cities, so these problems can be overcome by careful planning by relevant authorities.

Acknowledgments We acknowledge the Sentinel-5 satellite, Terra satellite and MODIS sensor and personnel and scientists for their efforts and data sharing and for the production.

Compliance with ethical standards

Competing interests The authors declare that there is no conflict of interest.

References

- Bart S, Nandin ET, Andreas V, Johannes R (2020) Mapping wetland characteristics using temporally dense Sentinel-1 and Sentinel-2 data: a case study in the St. Lucia wetlands, South Africa. *Int J Appl Earth Obs Geoinf* 86:141–189. <https://doi.org/10.1016/j.jag.2019.102009>
- Blosch G, Parajka J (2008) The value of MODIS snow covers data in validating and calibrating conceptual hydrologic models. *J Hydrol* 14:240–258
- Cheung CW, He G, Pan Y (2020) Mitigating the air pollution effect? The remarkable decline in the pollution-mortality relationship in Hong Kong. *J Environ Econ Manag* (2020). <https://doi.org/10.1016/j.jem.2020.102316>
- Emre A, Akyu Z, Ormanc AS, Ensoyc AS, Orman AU (2005) Using MODIS snow cover maps in modeling snowmelt runoff process in the eastern part of Turkey. *Remote Sens Environ* 97:216–230
- Fan H, Zhao Ch, Yang Y (2020) A comprehensive analysis of the spatio-temporal variation of urban air pollution in China during 2014–2018. *Atmos Environ* 220:127–201. <https://doi.org/10.1016/j.atmosenv.2019.117066>
- Fouladi F, Bailey MJ, Patterson WB, Sioda M, Blakley IC, Fodor AA, Jones RB, Chen Z, Kim JS, Lurmann F, Martino C, Knight R, Gilliland FD, Alderete TL (2020) Air pollution exposure is associated with the gut microbiome as revealed by shotgun metagenomic

- sequencing. *Environ Int* 138. <https://doi.org/10.1016/j.envint.2020.105604>
- Ghorbani R, Mobasheri MR, Rahimzadegan M (2010) Capability of Modis sensing data for qualitative and quantitative analyzes of air quality in urban areas. *J Climatol Res* 34:1–14
- Ghorbani R, Mobasheri MR, Rahimzadegan M (2012) Rapid method in estimation of suspended particle concentration using modis sensor in Tehran. *Hakim Research Journal* 15(2)
- Golbaz S, Farzadkia M, Kermani M (2009) Survey of Tehran air sanitary quality in 2008 based on air quality index. *Iran Occup Health J* 6:12–45
- Govender P, Sivakumar V (2020) Application of k-means and hierarchical clustering techniques for analysis of air pollution: a review (1980–2019). *Atmos Pollut Res* 1:40–56. <https://doi.org/10.1016/j.apr.2019.09.009>
- Ibbetson A, Symonds P, Hutchinson E (2020) Data to support small area health impact modelling of air pollution in the United Kingdom. *Data Brief* 29(2020):105148
- Jeniffer S, Ch Z, Tanya L, Alderete C, Toledo-Corral F, Lurmann K, Berhane F, Gilliland D (2019) Associations of air pollution, obesity and cardiometabolic health in young adults: the Meta-AIR study. *Environ Int* 133:78–120. <https://doi.org/10.1016/j.envint.2019.105180>
- John R, Balmes MD (2019) Household air pollution from domestic combustion of solid fuels and health. *J Allergy Clin Immunol* 143:1979–1987. <https://doi.org/10.1016/j.jaci.2019.04.016>
- Joris K, Ommeren J (2020) Urban air pollution and time losses: evidence from cyclists in London. *Reg Sci Urban Econ* 81:52–78. <https://doi.org/10.1016/j.regsciurbeo.2019.103504>
- Julia C, Fussell F, Kelly J (2019) Oxidative contribution of air pollution to extrinsic skin ageing. *Free Radic Biol Med*. Available online 23 December 2019. <https://doi.org/10.1016/j.freeradbiomed.2019.11.038>
- Kabolizadeh M, Rangzan K, Mohammadi S (2000) Application of integration of Landsat-8 and Sentinel-2 satellite images in environmental monitoring. *Remote Sens Geogr Inf Syst Nat Resour* 3:53–71
- Kohavi R, Provost F (1998) Glossary of terms: editorial for the special issue on applications of machine learning and the knowledge discovery process. *J Mach Learn* 30:271–274. [https://doi.org/10.1016/S0146-6453\(00\)80006-8](https://doi.org/10.1016/S0146-6453(00)80006-8)
- Kristin A, Halskov Hansen M, Liu Zh, Wang S (2019) The hidden hazard of household air pollution in rural China. *Environ Sci Pol* 93:27–33. <https://doi.org/10.1016/j.envsci.2018.12.004>
- Kurata M, Takahashi K, Hibiki A (2020) Gender differences in associations of household and ambient air pollution with child health: evidence from household and satellite-based data in Bangladesh. *World Dev* 128(2020):104779. <https://doi.org/10.1016/j.worlddev.2019.104779>
- Lalas D, Katsulis B, Petrakis M (1980) The contribution of the largest local emission sources of sulfur dioxide in Pireaus, Greece. *Hellenic Meteorol Soc Bull* 3:1–24
- Lesley G, Jeanine E, David R (2019) Detecting historic informal settlement fires with Sentinel 1 and 2 satellite data - two case studies in Cape Town. *Fire Saf J* 108(2019):102828. <https://doi.org/10.1016/j.firesaf.2019.102828>
- Li N, Chen G, Liu F, Mao S, Liu Y, Liu S, Mao Z, Lu Y, Wang C, Guo Y, Xiang H, Li S (2020) Associations between long-term exposure to air pollution and blood pressure and effect modifications by behavioral factors. *Environ Res* 182:109109. <https://doi.org/10.1016/j.envres.2019.109109>
- Lu M, Schmitz O, Vaartjes I, Karssenber D (2019) Activity-based air pollution exposure assessment: differences between homemakers and cycling commuters. *Health Place* 60. <https://doi.org/10.1016/j.healthplace.2019.102233>
- Matthias W, Jeroen S, Michael W, Hannes T (2020) Spatial and semantic effects of LUCAS samples on fully automated land use/land cover classification in high-resolution Sentinel-2 data. *Int J Appl Earth Obs Geoinf* 88. <https://doi.org/10.1016/j.jag.2020.102065>
- Miller MR (2020) Oxidative stress and the cardiovascular effects of air pollution. *Free Radic Biol Med*. <https://doi.org/10.1016/j.freeradbiomed.2020.01.004>
- Moon JK (2019) The effects of transboundary air pollution from China on ambient air quality in South Korea. *Heliyon* 5:196–205. <https://doi.org/10.1016/j.heliyon.2019.e02953>
- Mozaffari G, Narangi F, Haghghat Z (2015) Analysis of the relationship between synoptic patterns with particulate matter and carbon monoxide pollutants in Shiraz. *Geogr Environ Hazards* 14:95–115
- Nazarian A, Ziaecian P, Jangi AA (2007) Investigating the role of morphological location in Tehran air quality using GIS and satellite data (RS). *Geogr Res* 61:17–30
- Nolin A, Liang S (2000) Progress in bidirectional reflectance modeling and application for surface particulate media: snow and soil. *Remote Sens Rev* 14:307–342
- Oanh KT, Chutimon P, Ekbordin W, Supat W (2005) Meteorological pattern classification and application for forecasting air pollution episode potential in a mountain-valley area. *Atmos Environ* 39:1211–1225
- Omrani H, Omrani B, Parmentier B, Marco H (2020) Spatio-temporal data on the air pollutant nitrogen dioxide derived from Sentinel satellite for France. *Data Brief* 28:105089. <https://doi.org/10.1016/j.dib.2019.105089>
- Paola E, Veerle Buffel S, Bracke P (2019) Mental wellbeing, air pollution and the ecological state. *Health Place* 57:82–91. <https://doi.org/10.1016/j.healthplace.2019.03.003>
- Priya D, Barry P, Syed M (2020) Aggressive digital papillary adenocarcinoma and sentinel node biopsy: a case report and literature review. *JPRAS Open*. <https://doi.org/10.1016/j.jprou.2020.03.001>
- Purwadi I, van der Werff HMA, Lievens C (2020) Targeting rare earth element bearing mine tailings on Bangka Island, Indonesia, with Sentinel-2 MSI. *Int J Appl Earth Obs Geoinf* 88(2020):102055. <https://doi.org/10.1016/j.jag.2020.102055>
- Rangzan K, Kabolizadeh M, Rashidian M, Delfan H (2019) Modeling and zoning of water quality parameters using Sentinel-2 satellite imagery and computational intelligence (case study: Karun River). *Remote Sens Geogr Inf Syst Nat Resour* 4:2137
- Rohi G, Ejofodomi O, Ofualagba G (2020) Autonomous monitoring, analysis, and countering of air pollution using environmental drones. *Heliyon* 6(2020):e03252. <https://doi.org/10.1016/j.heliyon.2020.e03252>
- Safarianzengir V, Sobhani B (2020) Simulation and analysis of natural hazard phenomenon, drought in southwest of the Caspian Sea, Iran. *Carpathian J Earth Environ Sci* 15:127–136. <https://doi.org/10.26471/cjees/2020/015/115>
- Safarianzengir V, Sobhani B, Asghari S (2019) Modeling and monitoring of drought for forecasting it, to reduce natural hazards atmosphere in western and north western part of Iran, Iran. *Air Qual Atmos Health* 13:119–130. <https://doi.org/10.1007/s11869-019-00776-8>
- Sager L (2019) Estimating the effect of air pollution on road safety using atmospheric temperature inversions. *J Environ Econ Manag* 98:2019. <https://doi.org/10.1016/j.jeem.2019.102250>
- Saghafi MA, Aliakbari AA (2014) Investigation of circadian and seasonal variations of wind and air temperature and Co and PM10 contaminants in the atmosphere surface layer of Tehran City. *Spat Anal Environ Hazards* 1:17–34
- Sandro F, Pellegrini U (2004) Systematic analysis of meteorological conditions causing severe urban air pollution episodes in the central Po valley: 9th international conference on harmonization within atmospheric dispersion modeling for regulatory purposes. Garmisch-Partenkir, Germany, pp 1–4
- Schikowski T, Altug H (2020) The role of air pollution in cognitive impairment and decline. IUF-Leibniz Institute for Environmental

- Medicine, Duesseldorf, Germany, *Neurochem Int* 136:104708. <https://doi.org/10.1016/j.neuint.2020.104708>
- Shamsipour AA, Amini Z (2013) Simulation of co-dispersion pattern with Envi-met microclimatic model on Azadi-Tehran Pars Route. *Geogr Environ Hazards* 7:85–103
- Sobhani B, Safarianzengir V (2019a) Modeling, monitoring and forecasting of drought in south and southwestern Iran, Iran. *Model Earth Syst Environ* 5:63–71. <https://doi.org/10.1007/s40808-019-00655-2>
- Sobhani B, Safarianzengir V (2019b) Investigation hazard effect of monthly ferrin temperature on agricultural products in north bar of Iran. *Iraqi J Agric Sci* 50:320–330
- Sobhani B, Safarianzengir V (2020) Evaluation and zoning of environmental climatic parameters for tourism feasibility in northwestern Iran, located on the western border of Turkey. *Model Earth Syst Environ* 6:853–864. <https://doi.org/10.1007/s40808-020-00712-1>
- Sobhani B, Safarianzengir V, Kianian MK (2018) Potentiometric mapping for wind turbine power plant installation Guilan province in Iran. *J Appl Sci Environ Manag* 22:1363–1368. <https://doi.org/10.4314/jasem.v22i8.36>
- Sobhani B, Safarianzengir V, Kianian MK (2019a) Drought monitoring in the Lake Urmia basin in Iran. *Arab J Geosci* 12:448. <https://doi.org/10.1007/s12517-019-4571-1>
- Sobhani B, Safarianzengir V, Kianian MK (2019b) Modeling, monitoring and prediction of drought in Iran. *Iran (Iranica) J Energy Environ* 10: 216–224. <https://doi.org/10.5829/ijee.2019.10.03.09>
- Sobhani B, Safarianzengir V, Miridizaj F (2019c) Feasibility study of potato cultivating of Ardabil province in Iran based on VIKOR model. *Rev Agric* 10:92–102
- Sobhani B, Jafarzadehaliabad L, Safarianzengir V (2020a) Investigating the effects of drought on the environment in northwestern province of Iran, Ardabil, using combined indices, Iran. *Model Earth Syst Environ* 6:983–993. <https://doi.org/10.1007/s40808-020-00733-w>
- Sobhani B, Safarianzengir V, Yazdani MH (2020b) Modelling, evaluation and simulation of drought in Iran, southwest Asia. *J Earth Syst Sci* 129:100 (2020). <https://doi.org/10.1007/s12040-020-1355-7>
- Soltani T, Mofidi A, Gandomkar A (2015) Synoptic investigation of highly polluted days in Mashhad (case study: 13 and 14 November 2007). *J Spat Anal Environ Hazards* 4:95–112
- Song Y, Li M, Zhang M, Sun X (2019) Study on the impact of air pollution control on urban residents' happiness from microscopic perspective. *J Clean Prod* 229:1307–1318. <https://doi.org/10.1016/j.jclepro.2019.05.070>
- Susan MK, Africa F, Robert EG, Absae S, James N, Robinson M, Ashutosh L, Daniel EI (2018) Mapping threats to agriculture in East Africa: performance of MODIS derived LST for frost identification in Kenyas tea plantations. *Int J Appl Earth Obs Geoinf* 72: 131–139. <https://doi.org/10.1016/j.jag.2018.05.009>
- Tiwary A, Colls J (2010) Air pollution: measurement, modelling and mitigation, Third edn. Routledge, Taylor and Francis group, 528 p
- Tsolmon R, Ochirkhuyag L, Sternberg T (2008) Monitoring the source of trans-national dust storms in North East Asia. *Int J Digit Earth* 1: 119–129
- Vanino S, Nino P, De Michele C, Falanga Bolognesi S, D'Urso G, Di Bene C, Pennelli B, Vuolo F, Farina R, Pulighe G, Napoli R (2018) Capability of Sentinel-2 data for estimating maximum evapotranspiration and irrigation requirements for tomato crop in Central Italy. *Remote Sens Environ* 215:452–470. <https://doi.org/10.1016/j.rse.2018.06.035>
- Wan Z (1999) MODIS landsurface temperature algorithm theoretical basis document. Institute for Computational Earth System Science University of California Santa Barbara 3:1–77
- Wang L, Yuesi W, Jinyuan X, Zhanqing L, Xiaoyuan W (2010) Assessment and comparison of three years of Terra and Aqua MODIS Aerosol Optical Depth Retrieval (C005) in Chinese terrestrial regions. *Atmos Res* 97:229–240
- Wu Q, Lu J (2020) Air pollution, individual investors, and stock pricing in China. *Int Rev Econ Financ* 67:267–287. <https://doi.org/10.1016/j.iref.2020.02.001>

Publisher's note Springer Nature remains neutral with regard to jurisdictional claims in published maps and institutional affiliations.